Article:
Rosbottom, I, Pickering, JH, Hammond, RB et al. (1 more author) (2020) A Digital Workflow Supporting the Selection of Solvents for Optimizing the Crystallizability of p-Aminobenzoic Acid. Organic Process Research & Development, 24 (4). pp. 500-507. ISSN 1083-6160

https://doi.org/10.1021/acs.oprd.9b00261

A Digital Workflow Supporting the Selection of Solvents for Optimising the Crystallisability of Para Aminobenzoic Acid

Ian Rosbottom[δ], Jonathan H. Pickering, Robert B. Hammond, Kevin J. Roberts*

Centre for the Digital Design of Drug Products, School of Chemical and Process Engineering, University of Leeds, Woodhouse Lane, Leeds, LS2 9JT, UK

* Communicating Author email: k.j.roberts@leeds.ac.uk

δ new address: Department of Chemical Engineering, Imperial College London, South Kensington Campus, London, SW7 2AX

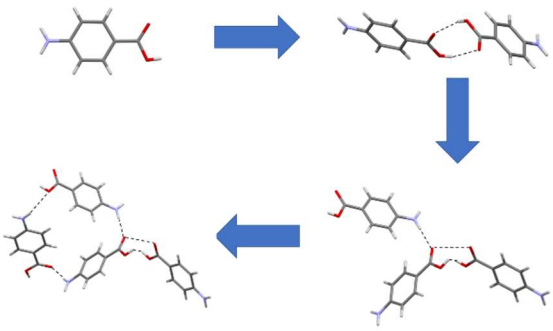

Build up of most stable four molecule cluster of *p*ABA from grid-based simulations

Abstract

We present a grid-based molecular modelling approach mechanics software for screening the solute-solvent and solute-solute interactions of organic molecules. This tool can provide some deeper understanding of solubilisation of organic molecules, intended to guide scientists to intuitive conclusions about whether a solute/solvent pair may provide the physical properties desired, such as crystallisability, solubility and crystal polymorphism.

The study focused on solutions of p-aminobenzoic acid in acetonitrile, ethanol and water. Acetonitrile molecules are found to form the weakest interactions with the solute molecule, although they also form weak interactions with themselves. In contrast, water forms strong interactions with the solute molecule, with strong preference to interact with the carboxylic acid group, although they also form strong self-interactions. Ethanol forms strong interactions with all of the solute molecule, along with reasonably strong interactions with itself.

The looser solvation of the carboxylic acid group by acetonitrile is thought to drive the crystallisation of the α polymorph, by lowering the crystallisation kinetic energy barrier. In ethanol the strong interactions of the solvent are thought to contribute to the significant undercooling of ethanolic solutions observed in previous studies. Water's strong interactions with the carboxylic acid of the solute may drive the self-assembly of the α-form by interactions of the phenyl groups, and also contribute to the nucleation of the β-form from this solvent.

This workflow can provide valuable guidance on the solvation properties of organic molecules and clusters, as well as producing low energy solvation shells of molecules and clusters to be utilised as starting points for more sophisticated simulations, such as molecular dynamics.

Keywords: Crystallisability, Molecular Modelling, Grid-based Modelling, Solubility, Solvation, Polymorphism

1. Introduction

The Made Smarter Review 2017[3] outlined the need for high value chemical industries, such as the pharmaceutical industry, to take greater advantage of digital technologies in their manufacturing workflows. The advances in first principles molecular modelling has seen the use of these tools in solubility screening,[4-6] the prediction of stable crystal structures[7] and morphology prediction.[8-10] Despite this, barriers to uptake of such tools can appear if the usability of the program is poor or the computations are too time consuming.

Crystallisation from solvent is the often-preferred method of purification of an organic small molecular active pharmaceutical material (API), as the crystalline form is the most stable and pure form of a material. The choice of solvent can be much more complex, since properties such as low solubility, polymorphism (different crystal structures of the same material) and particle size and shape can vary from solvent to solvent. Such properties need to be optimised to maximise the product performance in downstream processing for the manufacture of an efficacious product.

There are a variety of multi-scale techniques available to predict thermophysical data and solution chemistry, from *ab initio* calculations of full electronic structures[11, 12] through to more empirical based group contribution methods.[13] However, to capture the possible variety and detail of intermolecular interactions between the solute-solute, solute-solvent and solvent-solvent in the bulk solution and at the solution-surface interface, molecular mechanics (MM) and molecular dynamics (MD) simulations using interatomic force fields to calculate the interactions between molecules are often favoured.[14-18]

Whereas MD simulations can explore the dynamic motion of molecules in multiple states over small timescales, grid-based MM simulations sacrifice the molecular motion to rapidly identify the most favoured molecule-molecule[15, 16] or molecule-surface[17, 18] interactions by calculating interaction energies at user-specified grid-points (both spatial and rotational). Intermolecular grid-based molecular simulations have been effective for refining crystal structures from powder patterns[19], selecting co-crystal co-formers,[20] identifying solvent surface wetting impact upon crystal morphology[18, 21] and API-excipient compatibility.[22] These calculations have the advantage of running far more quickly than MD simulations, with typical run times of minutes or hours on a lap-top computer, compared with hundreds of hours for MD simulations.

The high speed allows the sampling of many possible intermolecular geometries of multiple systems, in the bulk solution and at the crystal-solution interface, which is attractive in industrial applications where rapid screening of multiple material properties is required. Such simulations can be used to target more advanced and computationally expensive simulations, or experimental work. Some molecular mechanics programs have been developed to assess

cluster stability[23] and search for solvation sites of proteins,[24, 25] however such approaches have yet to be incorporated into a workflow.

This paper presents a grid-based modelling approach to understanding the solute-solute, solute-solvent and solvent-surface interactions of *p*-aminobenzoic acid (*p*ABA)[1, 2] in acetonitrile (MECN), ethanol (EtOH) and water (H_2O). The favoured binding sites of *p*ABA with itself are predicted using a grid-based systematic search method to examine the lowest energy small clusters of *p*ABA. This is repeated to explore the solvent interactions with *p*ABA, gaining an understanding of how the molecule is likely to de-solvate from the above solvents and how this is likely to affect solute aggregation. This digital screening of solvation can be used as a guide to why a particular solvent may solvate a material well, with the computational efficiency to be potentially used on a large data set of solutes and solvents to conduct an initial screen of lead solute/solvent pairs for good solubility. In addition, we also demonstrate how this initial understanding could be extrapolated to provide basic insights into the nucleation and polymorphism in that solvent using these simple and computationally efficient simulations.

The crystal chemistry, solution chemistry, crystallisation and growth of the α- and β-polymorphic forms of *p*-aminobenzoic acid (*p*ABA) has been well investigated,[1, 2, 9, 26-32] both theoretically and experimentally. The high temperature stable α-form has been observed to dominate the crystallisation from most organic solvents,[2, 26, 29, 30, 33-35] even in conditions where the β-form is thought to be more thermodynamically stable. It has been proposed that the fast nucleation and physical properties of the α-form is driven by the stable OH…O H-bonding 'classic dimer' interactions and the unbroken chain of π-π stacking interactions along the long axis of the needle,[2, 9] leading to rapid nucleation and growth of this form into a needle. Hence, this wealth of experimental understanding of the solubility, nucleation and crystal growth makes this an attractive candidate for our proof of concept calculations of our digital screening tool.

2. Materials and Methods

2.1. Material: *p*-Aminobenzoic Acid

P-Aminobenzoic acid has two well-characterised polymorphs, α[27, 36, 37] and β,[27] recently a third polymorph[38] and a nitromethane solvate[32] have been discovered. The α- and β-*p*ABA structures have significantly different intermolecular structural chemistry and morphologies, see Figure 1.

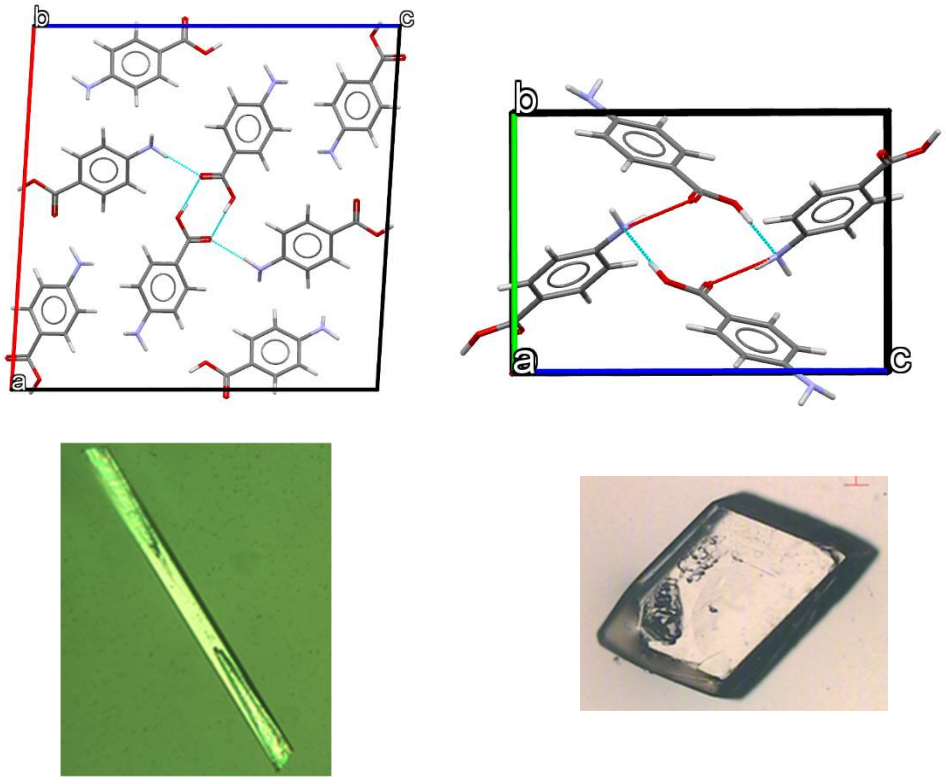

α-*p*ABA β-*p*ABA

Figure 1: The crystal packing of the α- and β-polymorphs[1, 2] of *p*ABA, and their crystal morphologies, α growing as a needle like form

The packing of the α-form is characterised by strong intermolecular OH…O and NH…O H-bonding interactions, along with an unbroken chain of π-π stacking interactions directed along the long-axis of the needle. In contrast, the packing of the β-form has a more isotropic structure with strong interactions in all three dimensions, where the combination of the ring of H-bonds and the head to tail π-π stacking interactions in these different direction produce a more block like crystal morphology[1, 2].

These two polymorphs share an enantiotropic relationship, with the α-form stable at high temperatures and the β-form at low temperatures. The thermodynamic transition temperature is believed to be between 14°C-17°C,[28, 33] however, solution crystallisation often yields needle-like α-crystals at temperatures below this range.

2.2. Computational Methods

2.2.1. Digital Workflow

The molecular interaction energy calculator (Mol-Mol) has been previously described in detail,[20] operates by taking two atom assemblies (usually but not necessarily molecules) in

fixed confirmations as input. One assembly is the target, around which a search grid is defined, the second assembly is the probe. During the calculation the probe is located at every point in the search grid, at each of which it is rotated through the points of an angular search grid. At every point in joint space and angular search the probe-target interaction energy is calculated by summing an interatomic potential, and an electrostatic potential, for all pairs of probe-target atoms. Finally, a low pass energy filter can be applied to remove interactions that are not significant or represent the physically impossible condition of a high energy probe target collision.

Solvation can be studied by using solute as the target, and solvent as the probe, with further data available from solute-solute and solvent-solvent studies. The program also has a cluster building mode in which probe molecules are located at low energy sites, in a precomputed grid around a target, allowing for probe-probe interactions. The software fits into a four-stage digital workflow for studying crystallization from solutions.

1. Construct, or extract from databases, probe and target molecules.
2. Calculate the atomic partial charges for both molecules.
3. Run Mol-Mol in solvent-solvent, solute-solvent and solute-solute modes.
4. Run Mol-Mol in cluster building mode for solute-solvent and solute-solute, and then optimize the clusters using any available molecular optimisation tool.

This workflow is intended to be a computationally efficient method to unpick explicit intermolecular interactions between solute and solvent to provide some guide to solvent dependent behaviour of organic molecules. Approaches such as COSMO-RS and group contribution methods can rapidly predict thermochemical data of solutions, however these lack the explicit intermolecular chemistry which can be displayed from molecular simulations. In contrast, MD simulations can calculate precise details of intermolecular solution chemistry and motion, but the computational expense is high, and the data analysis is challenging. All the simulations presented in this paper took less than one minute on a single processor.

2.2.2. Calculation of Intermolecular Interactions

All intermolecular interactions in this study were calculated using the Dreiding interatomic potential,[39] which is parameterised for a variety of organic molecules. The atomic partial charges were derived from a calculation of the electrostatic potential using Gaussian09, charges from electrostatic potentials using a grid based method (ChelpG) scheme,[40] using a 6-31G* basis set at the Becke, three parameter Lee Yang Par exchange correlation function.[41, 42] This approach has been extensively used when calculating intermolecular interactions of organic molecules in order to predict their physical properties.[9, 15, 20, 32, 43, 44]

2.2.3. Geometry Optimisation of Solvation Clusters

The geometry of the solvation clusters was optimised using the Forcite Module within Biovia's Materials Studio 8.0 package.[45] The SMART algorithm was used, with medium tolerance for the convergence. The Dreiding forcefield[39] and Gasteiger[46, 47] atom point charges were used in the calculation of the intra- and inter-molecular energies.

3. Results and Discussion

3.1. Single Molecule Solvation Search

The solvation sites for the single molecule of *p*ABA were calculated for MECN, EtOH and H_2O, increasing the energy filter (e.g. for an energy filter of -2kcal mol^{-1}, any solvent-*p*ABA interactions weaker than -2kca/mol are filtered out from the results) on each simulation, shown in Figure 2.

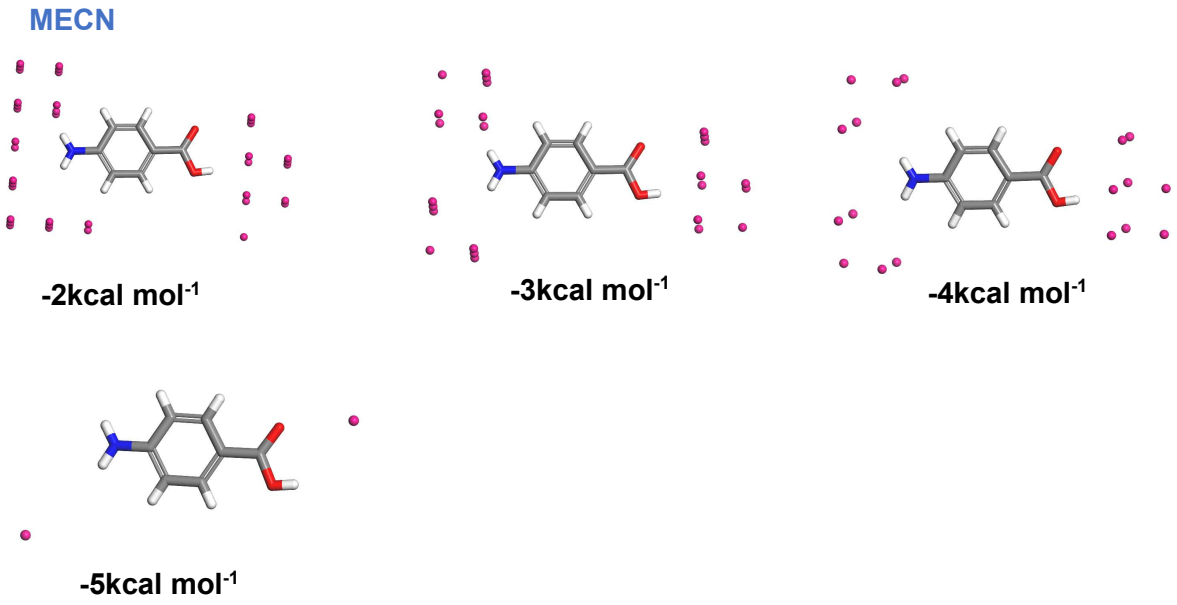

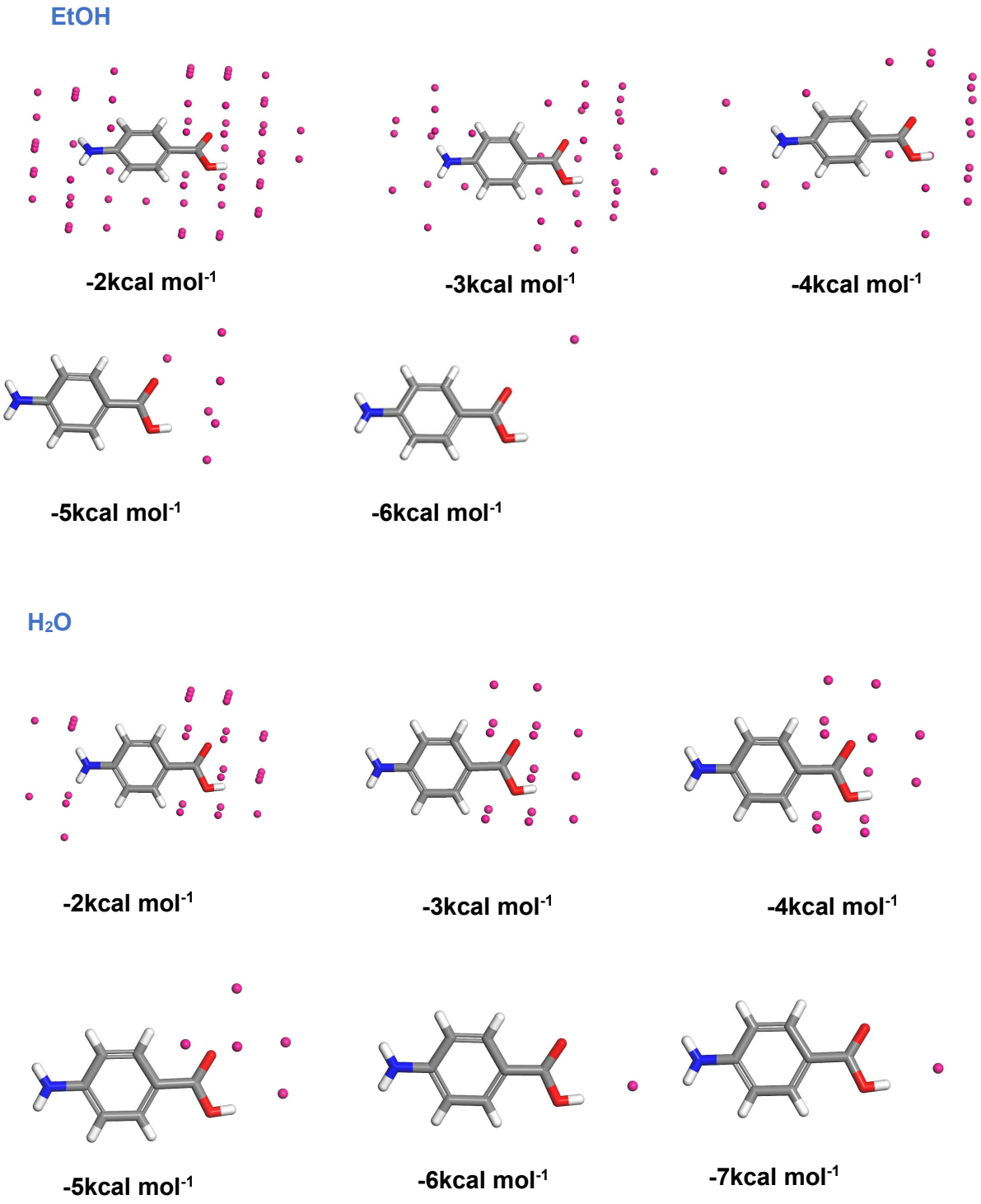

Figure 2: The strongest solvation sites for MECN, EtOH and H_2O interacting with *p*ABA using increasing energy filters from -2 to -7kcal mol^{-1}. Interactions that pass the energy filter are represented by a pink sphere. If no results are shown for the higher energy cut offs then this means that no results were found above the energy cut off

This tool gives a graphical representation of the most favoured solvent binding sites, where the increasing energy cut off can show which binding sites will quickly become de-solvated

and which are likely to need more energy to de-solvate. Figure 2 shows that for H_2O the strongest interactions are where the molecule can hydrogen-bond, which occurs around the COOH group. In comparison the H_2O, the software predicts MECN and EtOH can better solvate the NH_2 and phenyl ring groups, especially in the case of EtOH, which agrees with expectations. Indeed, it can also be observed that comparing MECN and EtOH, EtOH preferentially forms stronger interactions with the COOH group as well. The -4kcal mol^{-1} figures for these two solvents show a relatively similar number of spheres around the PABA molecule, with more of the spheres concentrated around the NH_2 group for MECN and more of them concentrated on the COOH group for EtOH. However, once the energy filter is raised to -5kcal mol^{-1}, only two spheres are left for MECN and around 6 are left for EtOH, which are all concentrated on the COOH group.

EtOH's ability to better solvate the entirety of the *p*ABA molecule, rather than just the polar groups, correlates well to *p*ABA being found to have a significantly higher solubility in EtOH than MECN or H_2O.[26, 35] The energies of the solvation sites of H_2O and MECN were found to be relatively similar, with H_2O being calculated to better solvate the COOH group as it is a H-bonding donor and acceptor, whereas MECN was calculated to better solvate the NH_2 group due to it being only a H-bonding acceptor. Despite this, it is experimentally observed that *p*ABA's solubility in water is approximately an order of magnitude lower than its solubility in MECN.

3.2. Solute Clustering and Solvation Shells

The search function gives a very reasonable first approximation of the binding sites, without revealing much details into the chemistry of the binding or what the intermolecular chemistry of solute or solvent mediated clusters may look like. Hence energetically favourable clusters of solute and solvent were built to provide a greater understanding of the solvation of *p*ABA, but also to give some guidance on how the solvent may impact upon the polymorphism of the material.

3.2.1. Solute Clustering

Since the nucleation behaviour of the α-form is thought to be dominated by the favourable solid-state synthons in its crystal structure, a search for the most favoured geometry of a four-molecule cluster of *p*ABA was carried out. Figure shows the results, along with the unit cells of α- and β-*p*ABA.

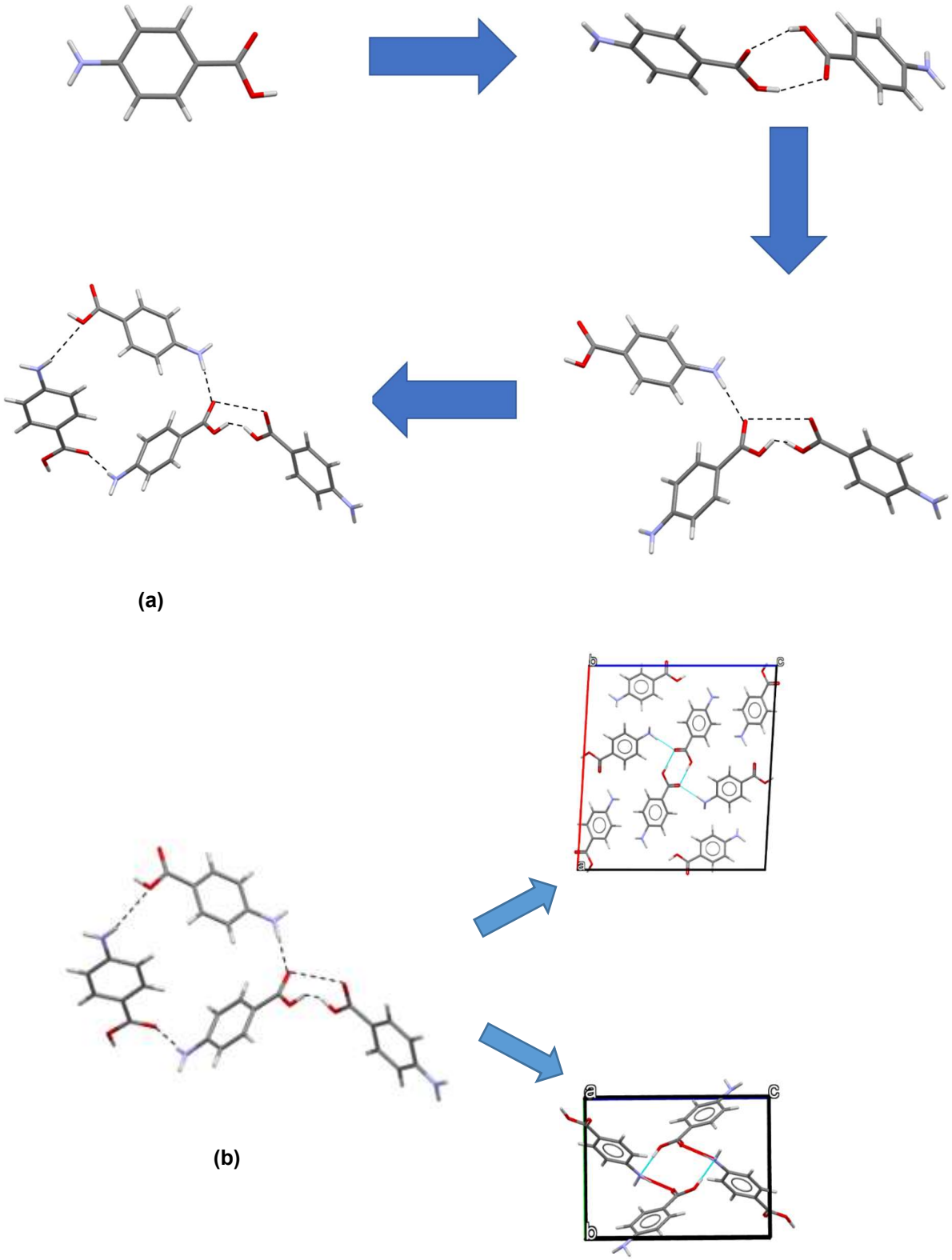

Figure 3: (a) The most energetically stable four molecule cluster of *p*ABA found from the grid based approach, showing how the molecules are sequentially added in energetically favourable geometries; (b) A comparison of the most stable four molecule cluster from the grid-based simulation to the unit cells of α- and β-*p*ABA, showing that this cluster more closely represents α-*p*ABA

Figure 3(a) shows that the most favoured solute-solute interaction from the Mol-Mol search is dominated by the OH…O H-bonds. This dimer is slightly more condensed than observed in the α-PABA crystal structure, likely due to the molecules maximising the dispersion interaction between the ring structures. The following additional interactions are the NH…O interactions. It is possible that the π-π ring stacking interactions are not seen from this search because of the orientation of the initial dimer forming some dispersion interactions with itself, hindering the formation of further such interactions with other molecules. This somewhat highlights a limitation of building clusters from this procedure.

Figure 3(a) shows that the four membered cluster, predicted by Mol-Mol, in solute-solute cluster mode, more closely resembles the solid-state structure of α-*p*ABA (Figure 3(b)), than that of β-*p*ABA (Figure 3(c)). Mol-Mol correctly finds the OH…O H-bonding dimer interactions and the NH…O interactions, which are typical of the solid-state structure of α-*p*ABA, which supports the hypotheses that the structure self-assembles through such building blocks. Though this simulation ignores any solvation effects, such as solvent molecules blocking otherwise favourable interactions, it does provide an indication of the preferred interactions of *p*ABA with itself.

3.2.2. Solvent Clusters

Figure 2 shows all the high energy solvation sites for *p*ABA with MECN, H_2O and EtOH, which have implications for solubility, solvent dependent nucleation kinetics and polymorphism. Water's preference for solvating the COOH group over any other part of a *p*ABA molecule suggests that in water the COOH group would be less available for solute-solute self-assembly, than in the other solvents. In contrast, Figure 2 shows that there was only one site where MECN has an interaction with the COOH group of PABA which was stronger than -5kcal mol^{-1}. This suggests that the work to de-solvate the COOH group in MECN would be much less than in H_2O, consistent with the dominance of the crystallisation of the α-form from this solvent, whereas the β-form can be crystallised from H_2O.

Further to this, Mol-Mol was used to predict ten molecule solvation shells around single molecules of *p*ABA. Since the clusters were built on a rigid grid, they were subsequently geometry optimised to find their lowest energy configurations. The results are shown in Figure 4 and the energies in Table 1.

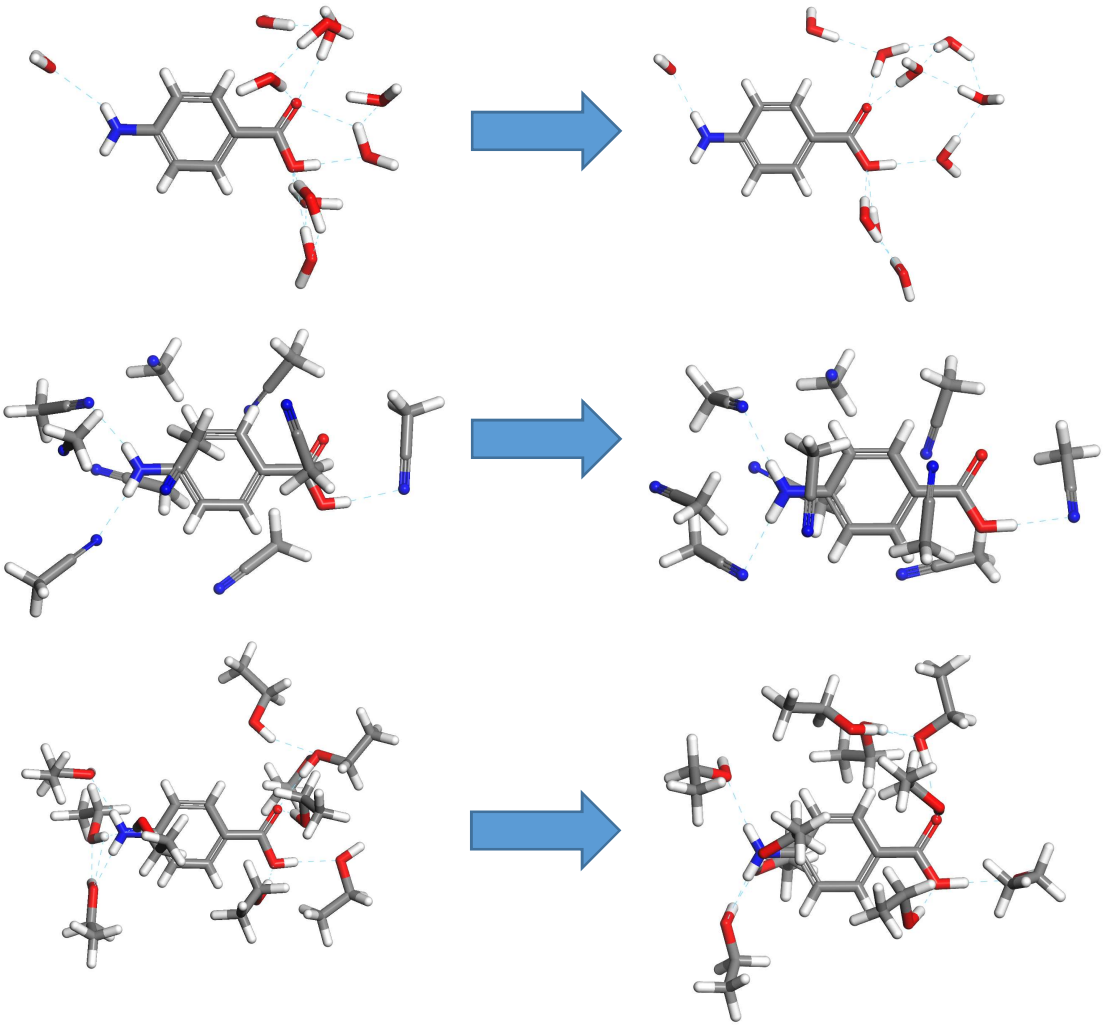

Figure 4: Ten molecule solvent clusters of H_2O (top), MECN (middle) and EtOH (bottom) around the *p*ABA molecule, broken down into solute/solvent and solvent/solvent interactions. Left of the arrows show clusters before geometry optimisation and right of the arrow after

Table 1: Total intermolecular interaction energies, per mole of solvent, for the ten molecule solvation clusters of PABA with H_2O, MECN and EtOH, split into solute-solvent and solvent-solvent interactions. Each solvent is listed twice the first result is the raw cluster builder, and the second is the optimised cluster. In general optimisation has increased the proportion of the total energy accounted for by solvent-solvent interactions

	Energy (kcal mol^{-1})		
Solvent	**Total**	**Solute-Solvent**	**Solvent-Solvent**
H_2O	-53.7	-33.7 (62.8%)	-20.0 (37.2%)
H_2O (Optimised)	-46.5	-21.0 (45.1%)	-25.5 (54.9%)
MECN	-29.2	-23.8 (81.5%)	-5.4 (18.5%)
MECN (Optimised)	-36.0	-20.9 (58.2%)	-15.1 (41.8%)
EtOH	-54.9	-39.7 (72.2%)	-15.3 (27.8%)
EtOH (Optimised)	-64.9	-42.5 (65.4%)	-22.4 (34.6%)

Figure 4 shows that the ten molecule solvation shells of MECN and EtOH form a more isotropic distribution around the *p*ABA molecule, whereas H_2O forms 9 of its 10 interactions with *p*ABA around the COOH group. This lack of isotropic solvation of H_2O around PABA could account for the low solubility of *p*ABA in this solvent. However, it must be observed that the solute-solvent interactions calculated for H_2O were found to be higher than the same for MECN. Relaxing the clusters into lower energy configurations by geometry optimisation had the effect of increasing the proportion of the total energy accounted for by the solvent-solvent interactions. This is a result of the cluster builder being driven a depth first search of the probe-target grid, so solvent molecules already located are fixed with solvent-solvent interactions only adjusting the location of solvents added later. Also, geometry optimisation has favoured the water molecules re-arranging to interact more strongly with themselves, in comparison to the MECN and EtOH clusters which remain broadly in the same structure.

However, a deeper comparison of the solute-solute and solute-solvent interactions found that H_2O had the strongest solvent-solvent interactions. It was also found that from the total intermolecular energy of the clusters, the solvent-solvent interactions accounted for

approximately 55% of the interaction energy for the water shell. In comparison, the solvent-solvent interactions only accounted for approximately 42% of the interactions in the MECN solvent shell. This indicates that water molecules provide a greater competition to the solute molecules for interaction than acetonitrile molecules, which may explain *p*ABA's significantly higher solubility in MECN than H_2O.

3.3. Implications on Crystallisability

These calculations of solute-solvent interactions and shells have provided qualitative backing for the chemical intuition about the solvent-solute interactions occurring in solutions of *p*ABA. However, the preferred positions found in the solvent-solvent simulations can also give insights into how *p*ABA molecules structure in solution, and how this can affect crystal nucleation and polymorphism.

The clusters constructed for MECN and EtOH showed that these molecules form a tight shell around a *p*ABA molecule, finding interactions with all parts of the *p*ABA molecule. In experiments these two solvents have only been observed to produce the α-form of *p*ABA, with the nucleation kinetic energy barrier being found to be lower for MECN than EtOH. Further to this, small angle X-ray scattering measurements of supersaturated ethanolic solutions of *p*ABA have identified denser phases in the solution which were estimated to be in the range of 100s of nanometres.[2]

The calculations and experimental data together suggest that the stronger interactions that EtOH forms with *p*ABA, and with itself, result in the formation of more stable solute rich phases in the bulk solution, which remain stable during significant undercooling.[2, 35] There is some debate as to whether the first critical step in the crystallisation of the α-form is the de-solvation of the carboxylic acid group, or aggregation driven by other parts of the molecule. Though we cannot draw definite conclusions from the simulations presented here, we think that it is pertinent that MECN demonstrates the loosest solvation around the COOH group, whilst EtOH clearly aggregates much more closely, implying that the de-solvation of the COOH group in EtOH would be much slower than in MECN, consistent with the nucleation kinetic data.[34, 35]

The crystallisation of *p*ABA has been observed to behave quite differently in aqueous solutions, in comparison to organic solvents.[30, 35, 48] Firstly, the nucleation of α-*p*ABA was observed to have almost none, or a very low, kinetic barrier to nucleation, whereby the solutions could hardly be undercooled.[35] Secondly, the often elusive β-polymorph was reliably crystallised at low supersaturations.[30, 48]

These calculations suggest that the water molecules poorly solvate a lot of the *p*ABA molecule preferring self-association, we believe this drives the progressive nucleation of α-*p*ABA with minimal undercooling. The strong interaction of water with the COOH group, along with the

strong network of solvent-solvent interactions that can form into an extended network away from the COOH group, appears to hinder the formation of the α-form; potentially even driving the self-association through stacking of the phenyl ring structures in this solvent, as theorised by Cruz-Cabeza et al.[48] Moreover, the head to tail stacking interaction is an important synthon in the β-structure, and this could also be the driving force for the nucleation of the β-form, observed in aqueous solutions.

3.4. Summary Discussion

Figure 5 provides a diagrammatic guide to impact of solvent on particle properties. The way in which the solvent molecules are attracted or repelled by the solute strongly impacts polymorphic form and morphology. For instance, the repulsion of water from the ring structure and its high affinity for the carboxylic acid group results in very thin α-PABA crystals and the appearance of the β-polymorph from this solvent only. This workflow is intended to be used in a cross-discipline setting, where the solvent impact on particle properties and the underpinning science must be transferred between people of different back grounds. We feel that such a diagram of the results could assist in the broader use of such modelling approaches in the pharmaceutical drug manufacture pipeline.

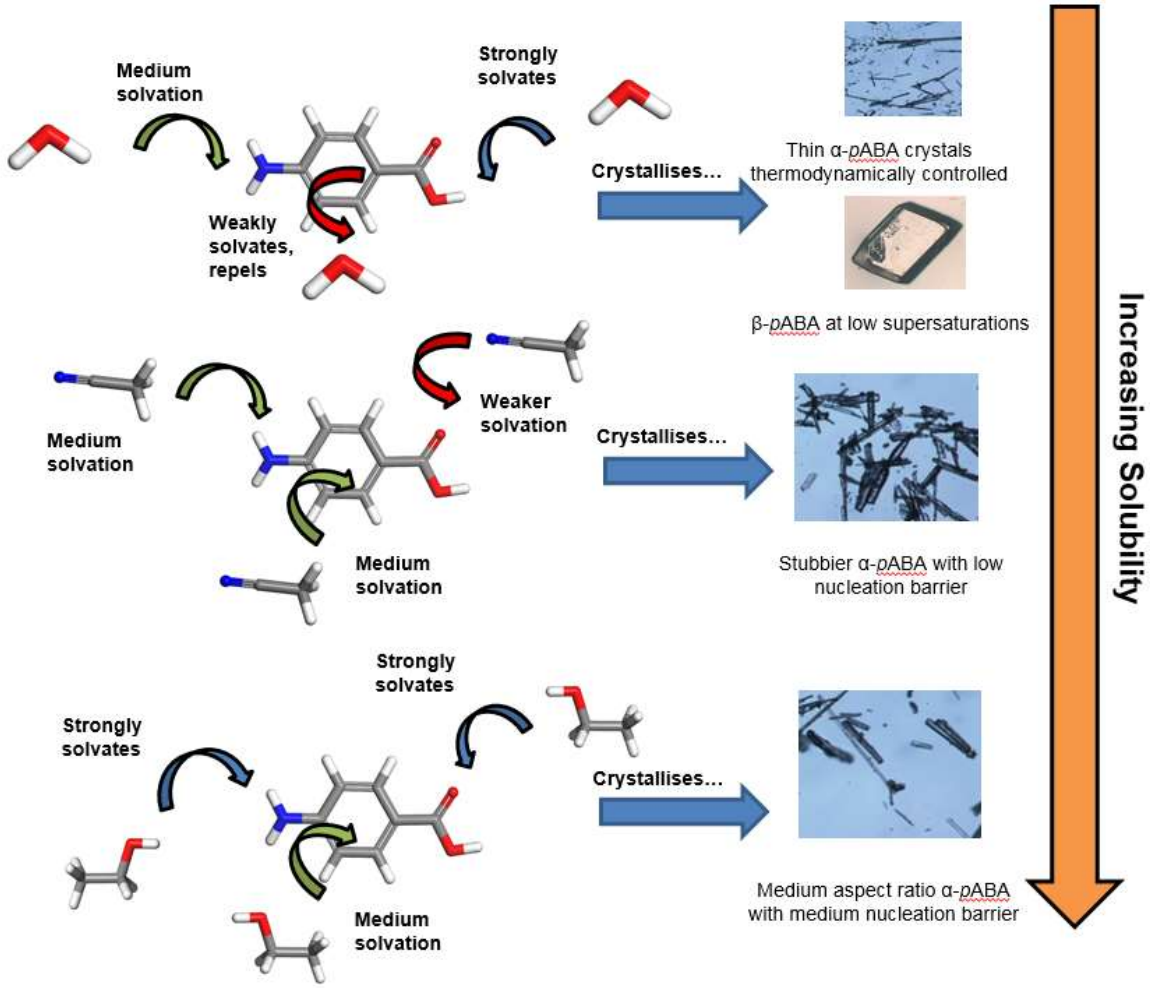

Figure 5: Proposed solvation mechanism of *p*ABA in (top to bottom) MECN, EtOH and H_2O. The blue arrows indicated strong solvation of the functional group by the solvent, then green as medium and red as weaker solvation

4. Conclusions

This study shows how the grid-based molecular modelling calculations of MECN, EtOH and H_2O provide an insight into the solubility and crystallisability of *p*ABA. These computationally efficient simulations provide a guide to the underlying chemistry of the well understood crystallisation behaviour of *p*ABA in MECN, EtOH and H_2O. We feel that this approach could find significant use if it could be adapted to screen multiple solutes and solvent, possibly using scripting approaches.

The utility of the method in a digital workflow arises from its computational speed; itself arising from the restriction of the probe to a search grid, with both probe and target being in fixed confirmations. This paper has demonstrated that this still allows good approximations of molecular behaviour to be made, with the final clustering results improved by the application

of geometrical optimisation, itself a relatively quick operation. Despite these simulations effectively being at zero kelvin, the preference of the solute-solute and solute-solvent interactions can give a good first approximation to the likely solution chemistry or intermolecular self-assembly. Such ensembles built from this workflow could be used as the starting point for MD simulations, which could provide more insight into how the solution concentration and temperature effects the solution chemistry.

Acknowledgements

We are grateful to the EPSRC for the support of crystallisation research at Leeds and Manchester through the award of a Critical Mass grant 'Molecules, Clusters and Crystals' (EP/I014446/1), which supported the PhD studies of one of us (I.R).[31] We also gratefully acknowledge the support of the Advanced Manufacturing Supply Chain Initiative through the funding of the 'Advanced Digital Design of Pharmaceutical Therapeutics' (Grant No. 14060) project in terms of supporting pharmaceutical crystallisation and modelling research at Leeds.

References

1. Sullivan, R. A.; Davey, R. J., Concerning the Crystal Morphologies of the alpha and beta polymorphs of p-aminobenzoic acid. *CrystEngComm* **2015,** *17*, 1015-1023.

2. Toroz, D.; Rosbottom, I.; Turner, T. D.; Corzo, D. M. C.; Hammond, R. B.; Lai, X.; Roberts, K. J., Towards an understanding of the nucleation of alpha-para amino benzoic acid from ethanolic solutions: a multi-scale approach. *Faraday Discussions* **2015,** *179*, 79-114.

3. Maier, J. *Made Smarter Review 2017*; 2017.

4. Klamt, A.; Eckert, F.; Hornig, M.; Beck, M. E.; Burger, T., Prediction of aqueous solubility of drugs and pesticides with COSMO-RS. *Journal of Computational Chemistry* **2002,** *23* (2), 275-281.

5. Klamt, A., Prediction of the mutual solubilities of hydrocarbons and water with COSMO-RS. *Fluid Phase Equilibria* **2003,** *206* (1-2), 223-235.

6. Docherty, R.; Pencheva, K.; Abramov, Y. A., Low solubility in drug development: de-convoluting the relative importance of solvation and crystal packing. *J. Pharm. Pharmacol.* **2015,** *67* (6), 847-856.

7. Price, S. L., Predicting crystal structures of organic compounds. *Chemical Society Reviews* **2014,** *43* (7), 2098-2111.

8. Dandekar, P.; Kuvadia, Z. B.; Doherty, M. F., Engineering Crystal Morphology. In *Annual Review of Materials Research, Vol 43*, Clarke, D. R., Ed. Annual Reviews: Palo Alto, 2013; Vol. 43, pp 359-386.

9. Rosbottom, I.; Roberts, K. J.; Docherty, R., The solid state, surface and morphological properties of p-aminobenzoic acid in terms of the strength and directionality of its intermolecular synthons. *CrystEngComm* **2015,** *17* (30), 5768-5788.

10. Hooper, D.; Clarke, F. C.; Docherty, R.; Mitchell, J. C.; Snowden, M. J., Effects of crystal habit on the sticking propensity of ibuprofen-A case study. *International Journal of Pharmaceutics* **2017,** *531* (1), 266-275.

11. Di Tommaso, D., The molecular self-association of carboxylic acids in solution: testing the validity of the link hypothesis using a quantum mechanical continuum solvation approach. *CrystEngComm* **2013,** *15* (33), 6564-6577.

12. Di Tommaso, D.; Watson, K. L., Density Functional Theory Study of the Oligomerization of Carboxylic Acids. *The Journal of Physical Chemistry A* **2014,** *118* (46), 11098-11113.

13. Tomoshige, N.; A., T. E.; A., G. R.; C., C. K., A group contribution molecular model of liquids and solutions. *AIChE Journal* **1977,** *23* (2), 144-160.

14. Hamad, S.; Moon, C.; Catlow, C. R. A.; Hulme, A. T.; Price, S. L., Kinetic Insights into the Role of the Solvent in the Polymorphism of 5-Fluorouracil from Molecular Dynamics Simulations. *The Journal of Physical Chemistry B* **2006,** *110* (7), 3323-3329.

15. Hammond, R. B.; Roberts, K. J.; Smith, E. D. L.; Docherty, R., Application of a Computational Systematic Search Strategy to Study Polymorphism in Phenazine and Perylene. *The Journal of Physical Chemistry B* **1999,** *103* (37), 7762-7770.

16. Hammond, R. B.; Hashim, R. S.; Ma, C.; Roberts, K. J., Grid-based molecular modeling for pharmaceutical salt screening: Case example of 3,4,6,7,8,9-hexahydro-2H-pyrimido (1,2-a) pyrimidinium acetate. *Journal of Pharmaceutical Sciences* **2006,** *95* (11), 2361-2372.

17. Hammond, R. B.; Pencheva, K.; Roberts, K. J., A Structural−Kinetic Approach to Model Face-Specific Solution/Crystal Surface Energy Associated with the Crystallization of Acetyl Salicylic Acid from Supersaturated Aqueous/Ethanol Solution. *Cryst Grow Des* **2006,** *6* (6), 1324-1334.

18. Hammond, R. B.; Pencheva, K.; Ramachandran, V.; Roberts, K. J., Application of grid-based molecular methods for modeling solvent-dependent crystal growth morphology: Aspirin crystallized from aqueous ethanolic solution. *Crystal Growth & Design* **2007,** *7* (9), 1571-1574.

19. Hammond, R. B.; Jones, M. J.; Roberts, K. J.; Kutzke, H.; Klapper, H., A structural study of polymorphism in phenyl salicylate: determination of the crystal structure of a meta-stable phase from X-ray powder diffraction data using a direct space systematic search method. *Zeitschrift Fur Kristallographie* **2002,** *217* (9), 484-491.

20. Hammond, R. B.; Ma, C.; Roberts, K. J.; Ghi, P. Y.; Harris, R. K., Application of Systematic Search Methods to Studies of the Structures of Urea−Dihydroxy Benzene Cocrystals. *The Journal of Physical Chemistry B* **2003,** *107* (42), 11820-11826.

21. Rosbottom, I.; Pickering, J. H.; Etbon, B.; Hammond, R. B.; Roberts, K. J., Examination of inequivalent wetting on the crystal habit surfaces of RS-ibuprofen using grid-based molecular modelling. *Physical Chemistry Chemical Physics* **2018,** *20* (17), 11622-11633.

22. Ramachandran, V.; Murnane, D.; Hammond, R. B.; Pickering, J.; Roberts, K. J.; Soufian, M.; Forbes, B.; Jaffari, S.; Martin, G. P.; Collins, E.; Pencheva, K., Formulation Pre-screening of Inhalation Powders Using Computational Atom–Atom Systematic Search Method. *Molecular Pharmaceutics* **2014,** *12* (1), 18-33.

23. Rackers, J. A.; Wang, Z.; Lu, C.; Laury, M. L.; Lagardere, L.; Schnieders, M. J.; Piquemal, J. P.; Ren, P. Y.; Ponder, J. W., Tinker 8: Software Tools for Molecular Design. *J Chem Theory Comput* **2018,** *14* (10), 5273-5289.

24. Emsley, P.; Cowtan, K., Coot: model-building tools for molecular graphics. *Acta Crystallographica Section D-Biological Crystallography* **2004,** *60*, 2126-2132.

25. Emsley, P.; Lohkamp, B.; Scott, W. G.; Cowtan, K., Features and development of Coot. *Acta Crystallographica Section D-Biological Crystallography* **2010,** *66*, 486-501.

26. Gracin, S.; Rasmuson, Å. C., Polymorphism and Crystallization of p-Aminobenzoic Acid. *Crystal Growth & Design* **2004,** *4* (5), 1013-1023.

27. Gracin, S.; Fischer, A., Redetermination of the beta-polymorph of p-aminobenzoic acid. *Acta Crystallographica Section E-Structure Reports Online* **2005,** *61*, O1242-O1244.

28. Hao, H. X.; Barrett, M.; Hu, Y.; Su, W. Y.; Ferguson, S.; Wood, B.; Glennon, B., The Use of in Situ Tools To Monitor the Enantiotropic Transformation of p-Aminobenzoic Acid Polymorphs. *Org. Process Res. Dev.* **2012,** *16* (1), 35-41.

29. Sullivan, R. A.; Davey, R. J.; Sadiq, G.; Dent, G.; Back, K. R.; ter Horst, J. H.; Toroz, D.; Hammond, R. B., Revealing the Roles of Desolvation and Molecular Self-Assembly in Crystal Nucleation from Solution: Benzoic and p-Aminobenzoic Acids. *Crystal Growth & Design* **2014,** *14* (5), 2689-2696.

30. Black, J. F. B.; Davey, R. J.; Gowers, R. J.; Yeoh, A., Ostwald's rule and enantiotropy: polymorph appearance in the crystallisation of p-aminobenzoic acid. *CrystEngComm* **2015,** *17* (28), 5139-5142.

31. Rosbottom, I. The Influence of Molecular Interactions and Aggregation on the Polymorphism, Crystal Growth and Morphology of Para Amino Benzoic Acid. University of Leeds, Leeds, 2015.

32. Rosbottom, I.; Ma, C. Y.; Turner, T. D.; O'Connell, R. A.; Loughrey, J.; Sadiq, G.; Davey, R. J.; Roberts, K. J., Influence of Solvent Composition on the Crystal Morphology and Structure of p-Aminobenzoic Acid Crystallized from Mixed Ethanol and Nitromethane Solutions. *Crystal Growth & Design* **2017,** *17* (8), 4151-4161.

33. Svard, M.; Nordstrom, F. L.; Hoffmann, E.-M.; Aziz, B.; Rasmuson, A. C., Thermodynamics and nucleation of the enantiotropic compound p-aaminobenzoic acid. *CrystEngComm* **2013**.

34. Turner, T. D. Molecular self-assembly, nucleation kinetics and cluster formation associated with solution crystallisation. University of Leeds, Leeds, UK, 2015.

35. Turner, T. D.; Corzo, D. M. C.; Toroz, D.; Curtis, A.; Dos Santos, M. M.; Hammond, R. B.; Lai, X.; Roberts, K. J., The influence of solution environment on the nucleation kinetics and crystallisability of para-aminobenzoic acid. *Physical Chemistry Chemical Physics* **2016,** *18* (39), 27507-27520.

36. Lai, T. F.; Marsh, R. E., The crystal structure of p-aminobenzoic acid. *Acta Crystallographica* **1967,** *22* (6), 885-893.

37. Athimoolam, S.; Natarajan, S., 4-carboxyanilinium (2R, 3R)-tartrate and a redetermination of the mu-polymorph of 4-aminobenzoic acid. *Acta Crystallographica Section C-Crystal Structure Communications* **2007,** *63*, O514-O517.

38. Benali-Cherif, R.; Takouachet, R.; Bendeif, E.-E.; Benali-Cherif, N., The structural properties of a noncentrosymmetric polymorph of 4-aminobenzoic acid. *Acta Crystallographica Section C* **2014,** *70* (3), 323-325.

39. Mayo, S. L.; Olafson, B. D.; Goddard, W. A., Dreiding - A Generic Force-Field For Molecular Simulations. *J Phys Chem* **1990,** *94* (26), 8897-8909.

40. Breneman, C. M.; Wiberg, K. B., Determining atom-centered monopoles from molecular electrostatic potentials. The need for high sampling density in formamide conformational analysis. *Journal of Computational Chemistry* **1990,** *11* (3), 361-373.

41. Becke, A. D., A new mixing of Hartree–Fock and local density-functional theories. *The Journal of Chemical Physics* **1993,** *98* (2), 1372-1377.

42. Lee, C.; Yang, W.; Parr, R. G., Development of the Colle-Salvetti correlation-energy formula into a functional of the electron density. *Physical Review B* **1988,** *37* (2), 785-789.

43. Nguyen, T. T. H.; Rosbottom, I.; Marziano, I.; Hammond, R. B.; Roberts, K. J., Crystal Morphology and Interfacial Stability of RS-Ibuprofen in Relation to Its Molecular and Synthonic Structure. *Crystal Growth & Design* **2017,** *17* (6), 3088-3099.

44. Rosbottom, I.; Roberts, K. J., Crystal Growth and Morphology of Molecular Crystals. In *Engineering Crystallography: From Molecule to Crystal to Functional Form*, Roberts, K. J.; Docherty, R.; Tamura, R., Eds. Springer Netherlands: Dordrecht, 2017; pp 109-131.

45. Biovia, D. S. *Materials Studio 7.0*, San Diego, 2017.

46. Gasteiger, J.; Marsili, M., New Model For Calculating Atomic Charges In Molecules. *Tetrahedron Letters* **1978,** (34), 3181-3184.

47. Gasteiger, J.; Marsili, M., Iterative Partial Equalization Of Orbital Electronegativity - A Rapid Access To Atomic Charges. *Tetrahedron* **1980,** *36* (22), 3219-3228.

48. Black, J. F. B.; Cardew, P. T.; Cruz-Cabeza, A. J.; Davey, R. J.; Gilks, S. E.; Sullivan, R. A., Crystal nucleation and growth in a polymorphic system: Ostwald's rule, p-aminobenzoic acid and nucleation transition states. *CrystEngComm* **2018,** *20* (6), 768-776.